6548–6557 *Nucleic Acids Research, 2008, Vol. 36, No. 20* *Published online 16 October 2008*
doi:10.1093/nar/gkn703

Synthesis and investigation of the 5-formylcytidine modified, anticodon stem and loop of the human mitochondrial tRNA^{Met}

Hrvoje Lusic[1], Estella M. Gustilo[2], Franck A. P. Vendeix[2], Rob Kaiser[3], Michael O. Delaney[3], William D. Graham[2], Virginia A. Moye[2], William A. Cantara[2], Paul F. Agris[2,*] and Alexander Deiters[1]

[1]Department of Chemistry, [2]Department of Molecular and Structural Biochemistry, North Carolina State University, Raleigh, NC 27695 and [3]Dharmacon, 2650 Crescent Drive #100, Lafayette, CO 80026, USA

Received July 29, 2008; Revised September 28, 2008; Accepted September 29, 2008

ABSTRACT

Human mitochondrial methionine transfer RNA ($hmtRNA^{Met}_{CAU}$) has a unique post-transcriptional modification, 5-formylcytidine, at the wobble position-34 (f^5C_{34}). The role of this modification in $hmtRNA^{Met}_{CAU}$ for the decoding of AUA, as well as AUG, in both the peptidyl- and aminoacyl-sites of the ribosome in either chain initiation or chain elongation is still unknown. We report the first synthesis and analyses of the tRNA's anticodon stem and loop domain containing the 5-formylcytidine modification. The modification contributes to the tRNA's anticodon domain structure, thermodynamic properties and its ability to bind codons AUA and AUG in translational initiation and elongation.

INTRODUCTION

Mitochondria generate over 90% of the energy used by mammalian cells through oxidative phosphorylation. Thirteen proteins, components of the electron transfer chain and the ATP synthase, are the products of mitochondrial DNA. The synthesis of these proteins is carried out by a specific protein synthesizing machinery within this organelle. During the almost-three decades since the sequencing of the human mitochondrial genome (1), the mitochondrial genetic code has been found to differ significantly from the universal code. The human mitochondrial gene for the one methionine specific tRNA ($hmtRNA^{Met}_{CAU}$, where CAU is the anticodon) plays a unique role since it must provide the tRNA used for both the initiation of protein synthesis and the elongation of the protein chain by responding to the codon AUA, normally an isoleucine codon in the cytoplasm, as well as the universal methionine code, AUG. This is highly unusual since all cytoplasmic protein biosynthetic systems employ two different $tRNA^{Met}$ species, one for initiation and one for elongation, and both respond to the single methionine codon, AUG. Maternally inherited mutations in the gene of this tRNA, including an A_{37} to G_{37} mutation adjacent to the anticodon nucleosides that read the two codons (Figure 1), are responsible for some devastating diseases (2–5). Moreover, the $hmtRNA^{Met}_{CAU}$ has a unique modification, 5-formylcytidine (Figure 1), at the wobble position-34 (f^5C_{34}) seen only in one other tRNA, a bovine liver, cytoplasmic $tRNA^{Leu}$ with a f^5C_{34} further modified with a 2′*O*-methyl (6). Nothing, however, is known about the decoding characteristics of $tRNA^{Leu\ 5}_{f\ CmAA}$. Since its discovery in bovine and nematode mitochondrial $tRNA^{Met}$ in 1994 (7,8), f^5C_{34} also has been found in the mitochondrial $tRNA^{Met}$ of squids, frogs, chickens, rats and fruit flies (9–11). The contribution of the f^5C_{34} modification to the structure of the $hmtRNA^{Met}_{CAU}$, its role in the decoding of AUG and AUA and its possible participation in either chain initiation or chain elongation by this unique $tRNA^{Met}$ is still unknown.

We speculate that mitochondria have a unique mechanism to partition this single $hmtRNA^{Met}_{CAU}$ species between initiation and elongation. While a $tRNA^{Met}_{CAU}$ unmodified at the wobble position-34 can read AUG, we hypothesize that the 5-formyl modification allows one $tRNA^{Met}$ to expand codon reading to include recognition of the AUA codon in mitochondrial mRNAs. Toward proving the hypothesis that this wobble modification affords the single $tRNA^{Met}$ the ability to decode AUG and AUA, we are reporting the first synthesis of a 5-formylcytidine-modified RNA and the initial structural and biological

*To whom correspondence should be addressed. Tel: +1 919 515 6188; Fax: +1 919 515 2047; Email: Paul_Agris@ncsu.edu
Correspondence may also be addressed to Alexander Deiters. Tel: +1 919 513 2958; Fax: +1 919 515 5079; Email: Alex_Deiters@ncsu.edu

The authors wish it to be known that, in their opinion, the first two authors should be regarded as joint First Authors

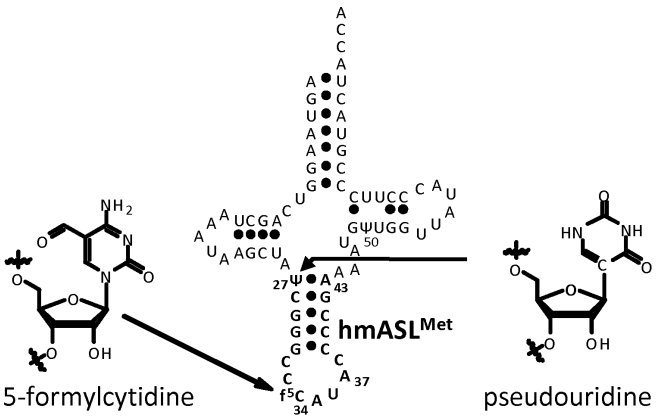

Figure 1. Human mitochondrial $tRNA^{Met}_{CAU}$. The sequence and secondary structure of $hmtRNA^{Met}_{CAU}$ are shown with the heptadecamer, anticodon stem and loop domain in bold. Nucleosides 27 and 50 are modified to pseudouridine, Ψ. The wobble position-34 modification is 5-formylcytidine, f^5C_{34}.

investigations. Previously, bovine mitochondrial $tRNA^{Met}_{CAU}$ had been shown to translate AUG and AUA in an *Escherichia coli* translational system *in vitro*, where AUG coded for methionine and AUA for isoleucine (12). However, site-specific binding was not investigated. Here we compare the codon binding affinities of the f^5C_{34}-modified anticodon stem and loop of human mitochondrial $tRNA^{Met}$ ($hmtASL^{Met}$-f^5C_{34}) with that of the unmodified ASL. Our results for both AUA and AUG codons at both the A and P-site of *E. coli* ribosomes increase our understanding of the modification's contributions to decoding and are consistent with previous results from the translation of poly(AUA) by bovine $mtRNA^{Met}_{CAU}$ on *E. coli* ribosomes (12).

MATERIALS AND METHODS

Experimental procedures and analytical data for the synthesis of the f^5C phosphoramidite (9)

All reagents used in the following experiments are of the highest purity and dryness possible. Before use, glassware was thoroughly cleaned and dried (oven at 110°C for 30 min). NMR analysis of intermediates was conducted in the appropriate deuterated solvent (referenced accordingly for $CDCl_3$: ^1H 7.24 p.p.m., ^{13}C 77.23 p.p.m.; and CD_3CN: ^1H 1.94 p.p.m.) using a Bruker Avance Ultrashield 300 MHZ spectrometer. Phosphorus, ^{31}P, NMR experiments were referenced according to an external H_3PO_4 standard (0.00 p.p.m.). Mass-spec analysis of the samples was performed on a Micromass LCT ESI-TOF or an Agilent LC-TOF. Analytes were dissolved in acetonitrile and flown against a Leucin Enkephalin lock mass standard. Chemical and physical properties of the intermediates were those of the expected compounds (Supplementary Data).

2′,3′-O-isopropylidenecytidine (2). To a suspension of cytidine (**1**, Figure 2, 1 g, 4.1 mmol) in 50 ml of acetone was added 2,2-dimethoxypropane (6 ml, 5.1 g, 49 mmol). $HClO_4$ was then added dropwise until the solution turned clear. The reaction mixture was stirred at room temperature for 12 h, after which it was neutralized by addition of $Ca(OH)_2$, filtered and evaporated. Purification by silica gel chromatography using $CHCl_3$: MeOH (80 : 20) with 2% TEA, afforded 966 mg of **2** as a white foam (83% yield). The analytical data obtained matched known literature data for **2** (13).

5-(Hydroxymethyl)- 2′, 3′-O-isopropylidenecytidine (3). To a solution of **2** (Figure 2, 1 g, 3.5 mmol) in 15 ml of 0.5 M KOH was added paraformaldehyde (1.05 g, 35 mmol). The reaction was stirred at 55°C for 36 h, after which it was cooled to room temperature and neutralized with 6 M HCl. The solution was filtered and evaporated. The oily residue was dissolved in MeOH : DCM (40 : 60), filtered and evaporated again. Purification by silica gel chromatography using MeOH : DCM (gradient 3 : 97, 8 : 92, 12 : 88) with 2% TEA, afforded 416 mg of 5-(hydroxymethyl)-2′,3′-*O*-isopropylidenecytidine (**3**) as a white foam (38% yield, 60% yield based on 357 mg of recovered starting material 2′,3′-*O*-isopropylidenecytidine (**2**).

5-Formyl-2′,3-O-isopropylidenecytidine (4). To **3** (Figure 2, 100 mg, 0.32 mmol) in 3 ml dioxane was added 500 mg ruthenium dioxide hydrate (five weight equivalents). The reaction mixture was refluxed for 12 h and filtered. Purification by silica gel chromatography MeOH : DCM (5 : 95) with 2% TEA, afforded 81 mg of the 5-formyl-2′,3′-O-isopropylidenecytidine (**4**) as a white solid (82% yield).

5-Formylcytidine (5). The acetonide, 5-formyl-2′,3′-O-isopropylidenecytidine (**4**, Figure 2, 500 mg, 1.61 mmol) was suspended in 1 M HCl (15 ml) at room temperature. The reaction progress was monitored by TLC. Upon disappearance of the starting material, the solution was neutralized with TEA. Water was subsequently evaporated. Recrystalization from MeOH afforded 414 mg of f^5C (**5**) as a white solid (95% yield).

N^4-[(Diisobutylamino)methylidene]-3′,5′-O-(1,1,3,3-tetraisopropyl-1,3-disiloxanediyl)-5-formylcytidine (6). 5-Formylcytidine (**5**, Figure 2, 0.47 g, 1.72 mmol) was dissolved in a mixture of 20 ml of pyridine and 2 ml of DMF. The solution was cooled to 0°C and $TIPDSCl_2$ (0.59 g, 1.89 mmol) in 2 ml of pyridine was added dropwise over a period of 1 h. The reaction was allowed to gradually warm to room temperature overnight. The following morning the reaction was quenched with 5 ml of MeOH and evaporated to dryness. The resulting paste was coevaporated twice with 20 ml of toluene and the crude material was purified by flash chromatography on 30 ml of silica gel using a gradient of MeOH in DCM (3–4%). Product fractions were pooled and evaporated to afford the TIPDS protected intermediate (0.88 g, 100%) as light yellow oil that is contaminated with residual pyridinium salts. The above compound was used as is without further purification to remove the residual pyridinium salts. TIPDS protected f^5C (**5**) (0.88 g, 1.72 mmol) was dissolved

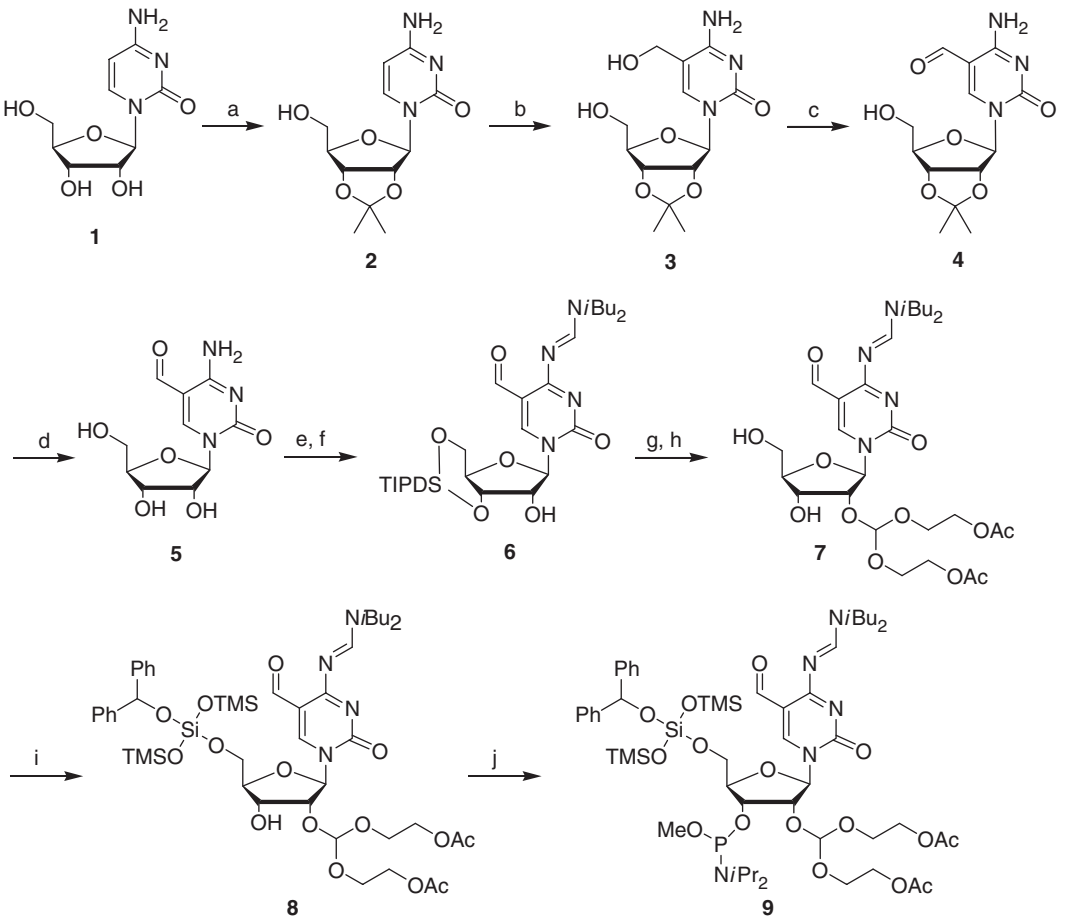

Figure 2. Synthesis of the 5-formylcytidine phosphoramidite. The starting compound cytidine is numbered compound **1**, intermediates are numbered **2–8** and the protected f^5C phosphoramidite is compound **9**. The synthetic transformations are: (**a**) acetone, dimethoxypropane, cat $HClO_4$ (83%); (**b**) paraformaldehyde, 0.5 M KOH, 55°C (38%, 60% brsm); (**c**) RuO_2 xH_2O, dioxane, reflux (82%); (**d**) 1 M HCl (95%); (**e**) $TIPDSCl_2$, Pyr, DMF; (**f**) DBF-$CH(OMe)_2$, DMF (71% over 2 steps); (**g**) ACE-orthoester, PPTS, TBDMS-pentanedione, DCM; (**h**) HF-TEMED, CH_3CN (53% over 2 steps); (**i**) BZH-Cl, DIA, DCM (84%); (**j**) $P(OMe)(DIA)_2$, DIA, S-Et Tetrazole, DCM (93%).

in 20 ml DMF and N,N-diisobutylformamidine dimethyl acetal (14) (0.70 g, 3.44 mmol) was added. The reaction was stirred for 16 h and evaporated under high vacuum. The resulting loose oil was coevaporated twice with 20 ml of toluene and the crude material was purified by flash chromatography on 30 ml of silica gel using a gradient of MeOH in DCM (1–2%). Product fractions were pooled and evaporated to afford 0.80 g of **6** as light yellow oil in 71% overall yield from f^5C (**5**).

2′-O-[Bis(2-acetoxyethoxy)methyl]-N^4-[(diisobutylamino) methylidene]-5-formylcytidine (7). A mixture of **6** (Figure 2, 0.80 g, 1.23 mmol), pyridinium para-toluenesulfonate (0.31 g, 1.23 mmol), and Tris(2-acetoxyethoxy)-methyl orthoformate (1.98 g, 6.15 mmol) was dissolved in 5 ml of DCM and stirred at room temperature. After 2 days, TBDMS-pentanedione (0.53 g, 2.46 mmol) was added and the reaction was stirred at ambient temperature. After stirring for an additional day, the reaction was quenched with 1 ml of TEMED. The crude material was separated from excess reagents by flash chromatography on 50 ml silica gel using a gradient of 25% ethyl acetate in hexanes with 0.1% TEMED to 50% ethyl acetate in hexanes with 0.1% TEMED. This material was concentrated to near dryness and taken directly onto the desilylation reaction.

A freshly made solution of TEMED (0.71 g, 6.15 mmol) in 10 ml of acetonitrile at 0°C was added 48% HF (0.15 ml, 4.30 mmol). This solution was allowed to stir for 5 min and added to the foregoing material from above at room temperature. The reaction was stirred for 2 h and concentrated to dryness. The crude material was purified by flash chromatography on 50 ml silica gel using a gradient of 20% heaxanes in ethyl acetate with 0.1% TEMED to 1% methanol in ethyl acetate with 0.1% TEMED. Product fractions were pooled and evaporated to leave the 2′-O-protected compound [**7**] as a light yellow oil (0.41 g) in 53% yield from the nucleobase protected compound **6**.

5′-O-[Benzyhydryloxy-bis(trimethylsilyloxy)silyl]-2′-O-[bis(2-acetoxyethoxy)-methyl]-N^4-[(diisobutyl-amino)-methylidene]-5-formylcytidine (8). Diisopropylamine (0.07 g, 0.65 mmol) was added to a solution of the 2′-O- and N^4-protected nucleoside, **7** (Figure 2, 0.41 g, 0.65 mmol) in 7 ml of DCM and the solution was cooled

to 0°C. In a separate flask BZHCl (0.34 g, 0.81 mmol) was diluted in 5 ml of DCM. Diisopropylamine (0.10 g, 0.98 mmol) was added to the silylating solution and the solution was allowed to stir for 2 min before being added dropwise to the nucleoside solution. The addition was completed within 30 min and the reaction was allowed to stir for 3 h and the reaction was quenched with 1 ml of MeOH and evaporated to dryness. The crude material was purified by flash chromatography on 30 ml silica gel using a gradient of 10% acetone in hexanes containing 0.1% (v/v) TEA to 20% acetone in hexanes containing 0.1% (v/v) TEA. Product fractions were pooled and evaporated to afford the 5′-O- protected compound **8** as a colorless oil. The yield was 0.56 g (84%).

5′-O-[Benzyhydryloxy-bis(trimethylsilyloxy)silyl]-2′-O-[bis(2-acetoxyethoxy)-methyl]-N^4-[(diisobutyl-amino) methylidene]-5-formylcytidine-3′-(methyl-N,N-diisopropyl) phosphoramidite (9). Bis(diisopropyl-amino) methoxy phosphine (0.21 g, 0.82 mmol) was dissolved in 3 ml of DCM and a 0.5-M solution of 5-ethylthio-1-H-tetrazole in anhydrous acetonitrile (0.08 ml, 0.55 mmol) was added. Diisopropylamine (0.06 g, 0.55 mmol) was then added and the phosphine solution was allowed to stir for 5 min at ambient temperature. In a separate flask, the 2′-O-, 5′-O- and N^4-protected f^5C, compound **8** (Figure 2, 0.56 g, 0.55mmol) and diisopropylamine (0.06 g, 0.55 mmol) were dissolved in 5 ml of DCM. The activated phosphine solution was added into the nucleoside solution and the reaction was stirred at room temperature. After 16 h the reaction was quenched with 2 ml of absolute ethanol and concentrated to dryness. The resulting white paste was purified by flash chromatography on 30 ml of silica gel using a mixture of DCM in hexanes [5 : 95 (v/v)] containing 2% (v/v) TEA followed by acetone in hexanes [1 : 9 (v/v)] to 2 : 8 (v/v) containing 0.5% (v/v) TEA. Product fractions were pooled and evaporated to afford the protected f^5C phosphoramidite **9** (Figure 2), as a colorless oil.

Polyribonucleotide synthesis of 5′-ΨCGGGCC-f^5C-AUA CCCCCGA-3′

The above sequence was synthesized on a 1-μmol scale using a ABI 394 DNA synthesizer using previously published procedures (15,16). The f^5C phosphoramidite (**9**, 0.067 M in anhydrous acetonitrile) was coupled to the growing polyribonucleotide chain for 3.5 min using 5-ethylthio-1H-tetrazole (0.5 M in anhydrous acetonitrile) as the activator. Once the synthesis of the polyribonucleotide chain was completed, the phosphate protecting groups were removed from the immobilized polyribonucleotide by treatment with disodium 2-carbamoyl-2-cyanoethylene-1,1-dithiolate trihydrate in DMF for 10 minutes. The support was washed excessively with water for 5 min and then flushed with Argon gas for 5 min to dry the support. The support was then transferred to a 2-ml Eppendorf tube and the polyribonucleotide was cleaved from the support and the exocyclic amine protecting groups were removed with 1 : 3 (v/v) tert-butylamine:water for 6 h at 60°C. The sample was cooled to room temperature, filtered and lyophilized to obtain the crude polyribonucleotide. The $hmASL^{Met}_{CAU}$ -Ψ_{27};f^5C_{34} was deprotected with acetate/TEMED according to standard Dharmacon protocols, purified by ion exchange HPLC (17), and dialyzed extensively against H_2O. The $hmASL^{Met}_{CAU}$-Ψ_{27} was synthesized and deprotected under standard conditions (18).

Confirmation of nucleoside composition by nucleoside HPLC and NMR of the $hmASL^{Met}_{CAU}$ constructs

Incorporation of f^5C modification within the $hmASL^{Met}$ was confirmed by NMR, including the two-dimensional NOESY (Figures 3 and 4). The nucleoside composition of the $hmASL^{Met}$ products was confirmed by enzymatic hydrolysis of the RNA to its constituent nucleosides (17) and then subjected to HPLC monitored by diode array UV spectrometry, the peaks identified, integrated and quantified (19) (Figure 4).

Analysis of thermodynamic stability, circular dichroism and molecular dynamics simulations

The ASL samples were dissolved to obtain a concentration of ~4 μM in 20 mM Na–K phosphate buffer (pH 6.8). UV-monitored, thermal denaturations and renaturations were replicated five times and monitored by measuring UV absorbance (260 nm) using a Cary 3 spectrophotometer as published (20,21). The data points were averaged over 20 s and collected four times a minute with a temperature change of 0.5°C/min from 4 to 90°C. The data were analyzed (22), and the thermodynamic parameters were determined (Origin software, Microcal, Inc.) (Figure 5A). CD spectral ellipticity data were collected using a Jasco 600 spectropolarimeter and an interfaced computer (Jasco, Inc.). $hmASL^{Met}_{CAU}$-Ψ_{27} or the $hmASL^{Met}_{CAU}$-Ψ_{27};f^5C_{34} (0.2 A260/ml, 20 mM Na–K phosphate buffer, pH 6.8) was placed in a temperature-regulated, 1-cm path-length quartz cell. Each sample was scanned 10 times at 25°C. The final data are an average of the 10 scans (Figure 5B). The molecular dynamics simulation (MDS) were performed by following standard published protocol (23) with the exception of using a truncated octahedral TIP3P water box (24).

Ribosomal binding assay

The 27-mer mRNA oligos used in codon binding assays were designed from that of T4 gp32 mRNA (25) and purchased (Dharmacon RNA Technologies). They were chemically deprotected and HPLC-purified in our lab. Each mRNA sequence was entered into the program RNA Structure 4.2 (26) and was found to have a low probability of folding into any stable conformation. The mRNA sequences are as follows (mitochondrial methionine codons AUA and AUG are in bold):

(i) 5′-GGCAAGGAGGUAAAA**AUA**GUAGCACG U-3′;
(ii) 5′-GGCAAGGAGGUAAAA**AUG**GUAGCACGU-3′;
(iii) 5′-GGCAAGGAGGUAAAAGUA**AUA**GCACG U-3′;

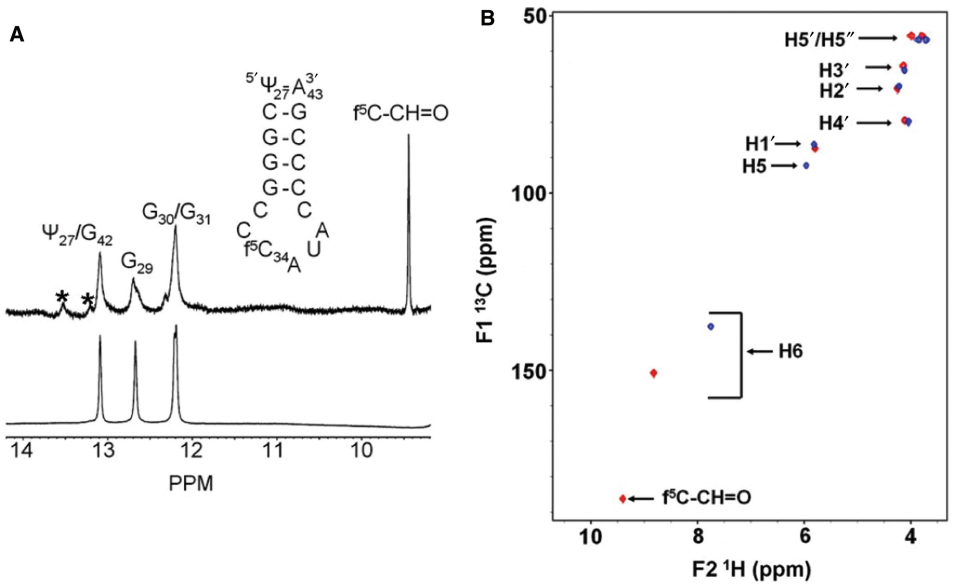

Figure 3. NMR spectra of the hmASL$^{Met}_{CAU}$. **(A)** One-dimensional 1H-NMR spectrum (in H_2O) of hmASL$^{Met}_{CAU}$-Ψ_{27};f^5C_{34} (top) is compared to that of the unmodified hmASL$^{Met}_{CAU}$-Ψ_{27} (bottom). The formyl proton's chemical shift in the RNA is almost identical to that of the mononucleoside f^5C. *Denotes impurities. **(B)** Superimposed ^1H-^{13}C HMQC spectra of cytidine (blue) and 5-formylcytidine (red).

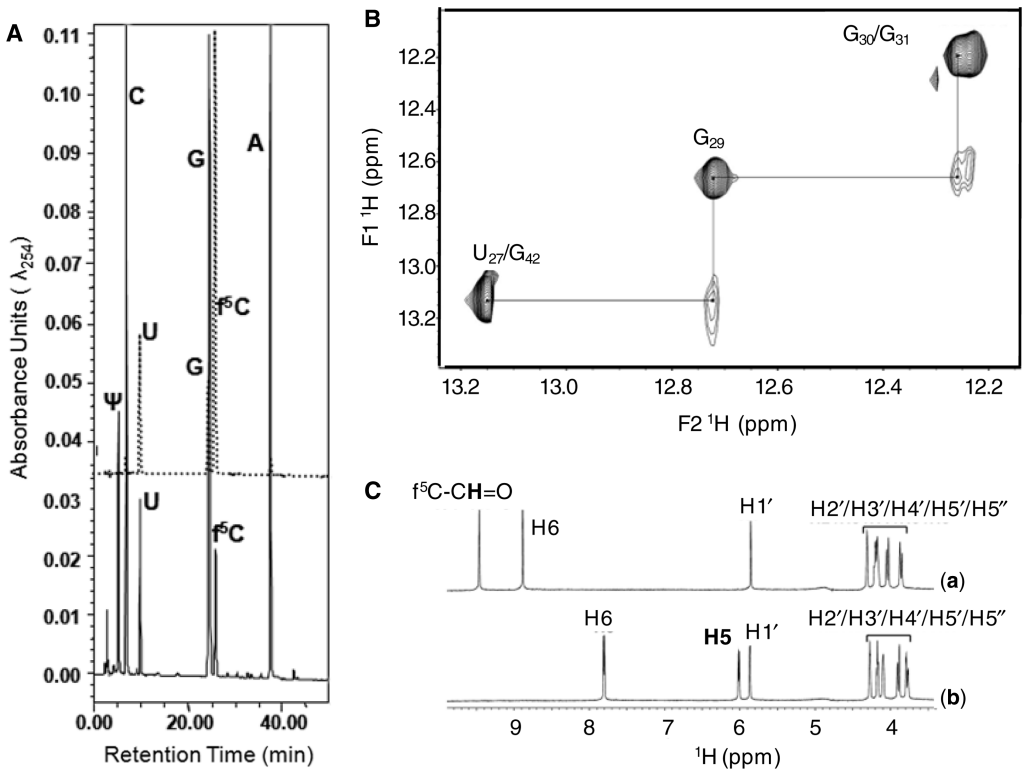

Figure 4. HPLC nucleoside composition and NMR analyses of hmASL$^{Met}_{CAU}$ and f^5C. **(A)** The upper section of the figure depicts the HPLC separation of standard ribonucleosides where C, G and A (solid line) had been injected together, and U, G and f^5C (dotted line) had been injected in a separate control experiment. The lower section depicts the chromatography of nucleoside composing the hmASL$^{Met}_{CAU}$ to include Ψ, as well as f^5C. **(B)** The NOESY connectivities between imino protons at 500 MHz in a 2D ^1H NOESY NMR spectrum (mix = 250 ms) of hmASL$^{Met}_{CAU}$ (90% ^1H_2O + 10% ^2H_2O; 20 mM PO_4^{3-}, 50 mM NaCl, pH 6.2; 2°C) with water suppression using the WATERGATE sequence. **(C)** 1D ^1H NMR spectra of (a) cytidine (**1**) and (b) 5-formylcytidine (**5**) (500 MHz; 100% ^2H_2O; 20 mM PO_4^{3-}, 50 mM Na^+, 50 mM K^+; pH = 6.2; 25°C) using the presaturation NMR sequence to suppress the water peak. The spectral regions and peaks corresponding to the various proton types in the molecules are labeled.

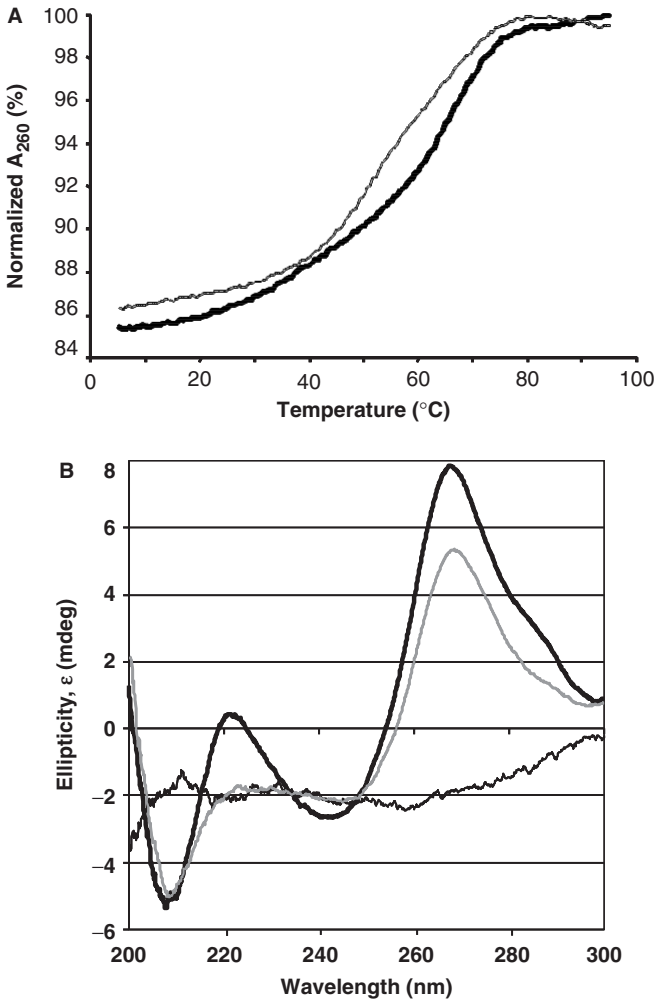

Figure 5. Thermal denaturations and circular dichroism spectra of the hmASL$^{Met}_{CAU}$-Ψ_{27} and the hmASL$^{Met}_{CAU}$-Ψ_{27};f^5C_{34}. **(A)** Thermodynamic stability of the ASLs. UV-monitored, thermal data were averaged from three denaturations and two renaturations for the hmASL$^{Met}_{CAU}$-Ψ_{27};f^5C_{34} (thin gray line) and for the hmASL$^{Met}_{CAU}$-Ψ_{27} (thick black line). **(B)** Circular dichroism spectra. Spectra of the hmASL$^{Met}_{CAU}$-Ψ_{27};f^5C_{34} (thin gray line) and that of the hmASL$^{Met}_{CAU}$-Ψ_{27} (thick black line) at the approximately equal concentrations of 2 μM were collected over the wavelength range of 200 to 300 nm.

(iv) 5′-GGCAAGGAGGUAAAAGUA**AUG**GCACG U-3′.

The 70S ribosomes were prepared from *E. coli* MRE600 (27). The ASLs were 5′-end ^{32}P-labeled using [ϒ-^{32}P] ATP (MP Biomedicals). Unlabeled ASLs (5 μM) were mixed with 10 000 CPM of 5′-end ^{32}P-labeled ASL. The assay was performed in ribosomal binding buffer (50 mM HEPES, pH 7.0; 30 mM KCl; 70 mM NH_4Cl; 1 mM DTT; 100 μM EDTA; 20 mM $MgCl_2$). The ribosomes, activated at 42°C for 10 min and then slowly cooled to 37°C, were then programmed with 2.5 μM mRNA for 15 min at 37°C. The ribosomal site not in observation was saturated with ASL$^{Val3}_{UAC}$ (unmodified) for 15 min at 37°C. P-site binding was performed prior to A-site binding. ASL$^{Val3}_{UAC}$ binds to the Val codon GUA; see underlined codons of the mRNA sequences above. Binding of ASL$^{Met}_{CAU}$ in either A- or P-site was allowed to proceed for 30 min at 37°C. The reaction mixtures (20 μl each) were then placed on ice for 20 min and filtered through nitrocellulose in a modified Whatman Schleicher and Schuell (Brentford, UK) 96-well filtration apparatus (28). Prior to filtration of experimental samples, the nitrocellulose filter was equilibrated in binding buffer at 4°C for at least 20 min and each well of the filtration apparatus was washed with 100 μl of cold binding buffer. Cold binding buffer (100 μl) was added to each sample, and the entire 120-μl volume was quickly filtered. Each well was then washed twice with 100 μl of cold binding buffer. The nitrocellulose was dried out on 'kim' wipes, and the radioactivity was measured using a phosphorimager (Molecular Dynamics, GE Healthcare). Data were measured for radioactive intensity using ImageQuant (Amersham). Nonspecific binding was determined by the binding of ASLs to ribosomes without mRNA and subtracted from the experimental data. The final data are a result of at least three separate experiments, each done with samples in triplicate, i.e. minimally nine determinations for each binding (Figure 6).

Analysis of the f^5C pKa

UV spectra were compiled (220–320 nm) using a Varian Cary3 Spectrophotometer at different pH values for cytidine and 5-formylcytidine. The spectra were normalized to 0.2 OD at 260 nm. Entire spectra were collected to ensure that they all intersected at 260 nm at an OD of ~0.2. However, the absorbance maximum at 280 nm was plotted against the pH, a previously published method of assessing the pKa of nucleosides (29). A pH range of 2.2–7.0 (citrate-phosphate buffer) was used for cytidine, and a pH range of 1.1–5.0 was used for f^5C (KCl–HCl buffer for pH values between 1.1 and 2.0 and citrate–phosphate buffer for pH values between 2.2 and 5.0). The line fitting and data analysis was conducted with Prism v3.00 (Graphpad Software, Inc.) (Figure 7).

RESULTS AND DISCUSSION

A 5-formylcytidine (f^5C) has previously been synthesized from 5-(hydroxymethyl)cytosine (13) and from 5-methyluridine (30), but not incorporated into an RNA sequence. First, we developed a short (four steps) and facile synthesis of f^5C (compound **5**, Figure 2) from commercially available cytidine (**1**, Figure 2), starting by protecting cytidine as the acetonide **2** under standard acid catalysis with an 83% yield. Installation of the hydroxymethylene unit occurred through an assisted Baylis-Hillman-type reaction with formaldehyde (**3**, 38% yield, 60% yield based on recovered starting material; Supplementary Data). Selective oxidation of the allylic alcohol with RuO_2 to the aldehyde **4** proceeded with an 82% yield. The acetonide protecting group was subsequently removed to deliver f^5C (**5**) in 95% yield. The comparison between the NMR signals of C and those of f^5C clearly demonstrated that the C-5 position of f^5C was substituted (Figures 3B and 4C). This substitution was further confirmed to be the formyl group by the presence of a low field shifted signal at (F1 = 185 p.p.m.;

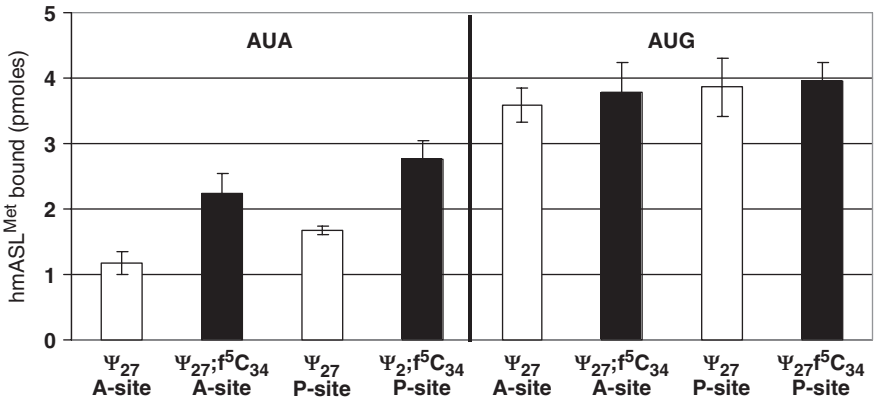

Figure 6. Codon binding by $hmASL^{Met}_{CAU}$-Ψ_{27} and the $hmASL^{Met}_{CAU}$-$\Psi_{27};f^5C_{34}$. The equilibrium binding of the two ASLs to the cognate and noncognate codons, AUG and AUA respectively, was assessed using programmed *E. coli* ribosomes. (The ASL unmodified and the wobble position is designated 'Ψ_{27}'; ASL modified at the wobble position is designated as '$\Psi_{27};f^5C_{34}$'.) The ASLs were bound to the A-site with *E. coli* ASL^{Val3}_{UAC} bound to its cognate codon in the P-site. The ASLs were bound to the P-site with the ASL^{Val3}_{UAC} bound to its cognate codon in the A-site.

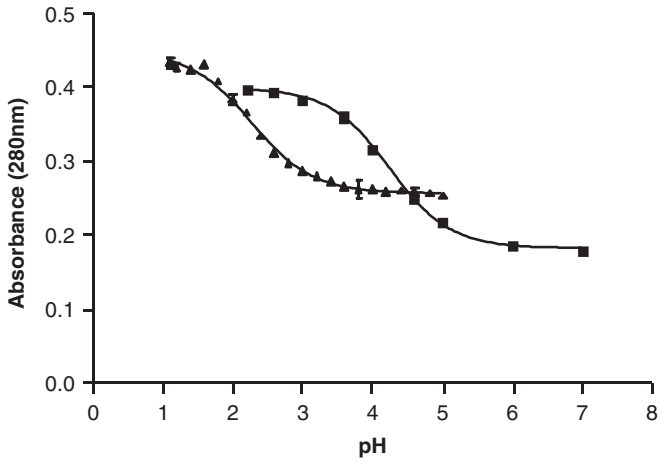

Figure 7. Analysis of the pKa of (filled squares) cytidine in comparison to that of (filled triangles) 5-formylcytidine. UV spectra were collected for the two nucleosides over a range of pH values, pH 2.2–7.0 for cytidine, and a pH 1.1–5.0 for f^5C. The absorbance at 280 nm was normalized and plotted against the pH.

F2 = 9.40 p.p.m.) corresponding to the CH group of the f^5C modification. A complete and unambiguous assignment of the non-exchangeable protons was achieved by using the two dimensional (2D) ^1H-^{13}C Heteronuclear Multiple Quantum Correlation (HMQC) method (31,32). As expected, the NMR peaks observed between (F1 = 50.00–85.00 p.p.m.; F2 = 4.50–6.00 p.p.m.) corresponded to the protons (H1′-H5′/H5″) of the ribose moiety (Figure 3B) (33). Conversion of f^5C into the 2′,5′-protected f^5C phosphoramidite (**9**, Figure 2) commenced with the protection of the 3′and 5′ hydroxyl groups as a disiloxane followed by protection of the 4-NH_2 group as the formamidine **6** (71% yield). Installation of a 2′-ACE orthoester [2′-O-bis(acetoxyethoxy)methyl-] followed by fluoride treatment delivered the diol **7** in 53% yield over two steps (15). The synthesis of the f^5C phosphoramidite **9** was completed through 5′-BZH (5′-O-benzhydroxy-bis (trimethylsiloxy)silyl-) protection (**8**, 84% yield) and phosphor-amidite formation (93% yield). A major concern for the incorporation of f^5C phosphoramidite into synthetic RNA oligomers was the formation of imine adducts with the formyl group under resin cleavage and deprotection conditions. However, we decided not to protect the formyl group since the final deprotection of the 2′-ACE groups under mildly acidic conditions would potentially hydrolyze any imine formation that results during base-deprotection back to the formyl group.

In order to investigate the contribution of f^5C_{34} to the structure of the anticodon loop and to the decoding of both the AUG and AUA codons at both the A- and P-sites, f^5C was incorporated into the anticodon stem and loop domain of $hmtRNA^{Met}_{CAU}$ ($hmASL^{Met}_{CAU}$) at the wobble position 34, along with pseudouridine, Ψ_{27}. The oligonucleotide was synthesized with Ψ_{27} and with and without f^5C_{34} ($hmASL^{Met}_{CAU}$-$\Psi_{27};f^5C_{34}$, and $hmASL^{Met}_{CAU}$-Ψ_{27}) using care not to oxidize the formyl group. Incorporation of f^5C into RNA was accomplished by activating with *S*-ethyl tetrazole and coupling of the activated species for 3.5 min to the growing polyribonucleotide on the solid-support. Cleavage from the support and deprotection of the exocyclic amines was tested using NH_4OH at room temperature for 24 h, methylamine at room temperature for 6 h, and *t*-butyl amine in water (1 : 3, v/v) at 60°C for 6 h. Only the *t*-butyl amine conditions resulted in the correct mass upon MALDI-TOF analysis of the crude products. There was no indication of any *t*-butyl-amine adducts present from the MALDI-TOF results. Successful incorporation of f^5C was confirmed by NMR measurements (Figures 3 and 4) and HPLC of constituent nucleosides (Figure 4). The proton resonance of the formyl group is observed in the low field region of the 1D spectrum of $hmASL^{Met}_{CAU}$-$\Psi_{27};f^5C_{34}$ and absent from that of the $hmASL^{Met}_{CAU}$-Ψ_{27} (Figure 3). The formyl proton in $hmASL^{Met}_{CAU}$-$\Psi_{27};f^5C_{34}$ resonates at the same chemical shift as that of the mononucleoside f^5C_{34}, as observed in the superimposed ^1H-^{13}C HMQC spectra of cytidine and 5-formylcytidine (Figure 3B). The HPLC

Table 1. Thermodynamic contributions of f^5C_{34}

$hmASL^{Met}_{CAU}$	T_m (°C)	ΔG°_{37} (kcal/mol)	ΔH (kcal/mol)	ΔS (cal/K·mol)	Hyperchromicity (%)
Ψ_{27}	67.7 ± 1.8	–2.8 ± 0.1	–31.1 ± 2.0	–91.3 ± 6.3	16 ± 1
$\Psi_{27};f^5C_{34}$	60.1 ± 0.8	–1.6 ± 0.1	–22.8 ± 1.2	–68.4 ± 3.4	16 ± 1

nucleoside composition analysis confirms the presence of the f^5C (Figure 4A).

The structure of the resulting $hmASL^{Met}_{CAU}$-$\Psi_{27};f^5C_{34}$ was characterized by 1D ^1H and 2D ^1H NOESY NMR experiments conducted in H_2O at 2°C (34), and by determining the thermodynamic contributions of f^5C to the RNA. The formyl proton resonance was found at 9.45 p.p.m. corresponding almost exactly to that of the nucleoside alone (Figure 3A). The imino protons of the stem of $hmASL^{Met}_{CAU}$-$\Psi_{27};f^5C_{34}$ were found to resonate between 12 and 13.5 p.p.m. on the ^1H 1D NMR spectrum (Figure 3A). The NMR spin systems that involve the exchangeable imino protons of $hmASL^{Met}_{CAU}$-$\Psi_{27};f^5C_{34}$ were identified by conducting NMR experiments in H_2O at 2°C (Figures 3A and Figure 4B). The identification and assignment of the exchangeable protons were indicative of the overall stability the $hmASL^{Met}_{CAU}$-$\Psi_{27};f^5C_{34}$ in solution, and the comparison with $hmASL^{Met}_{CAU}$-Ψ_{27} (Figure 3A) demonstrated the successful incorporation of f^5C_{34} into the sequence of $hmASL^{Met}_{CAU}$.

The modified RNA synthesis has allowed us to begin examining the role of f^5C_{34} in thermal stability and decoding activity of $hmtRNA^{Met}$. Thermodynamic parameters were extracted from the repeated denaturations and renaturations of both $hmASL^{Met}_{CAU}$-$\Psi_{27};f^5C_{34}$ and $hmASL^{Met}_{CAU}$-Ψ_{27} (Table 1 and Figure 5A). Introduction of f^5C_{34} lowered the melting temperature and standard free energy (ΔG°_{37}) considerably, but did not alter the ASL's hyperchromicity. The circular dichroism spectrum of the $hmASL^{Met}_{CAU}$-Ψ_{27} exhibited a greater ellipticity at 270 nm than that of the $hmASL^{Met}_{CAU}$-$\Psi_{27};f^5C_{34}$. The lower degree of ellipticity of $hmASL^{Met}_{CAU}$-$\Psi_{27};f^5C_{34}$ is indicative of a decrease in base stacking. The decreased base stacking must be attributed to the anticodon loop nucleosides because of the location of the modification. These differences in thermodynamics and circular dichroism ellipticity between $hmASL^{Met}_{CAU}$-$\Psi_{27};f^5C_{34}$ and $hmASL^{Met}_{CAU}$-Ψ_{27} indicated that f^5C_{34} may enhance the motional dynamics of the loop. This difference in motional dynamics was observed by a molecular dynamics simulation (MDS) performed on the $hmASL^{Met}_{CAU}$-Ψ_{27} and the $hmASL^{Met}_{CAU}$-$\Psi_{27};f^5C_{34}$ using AMBER 9 (35). The $hmASL^{Met}_{CAU}$-Ψ_{27} displayed an average root mean square deviation from the starting structure of 2.18 ± 0.23 as opposed to $hmASL^{Met}_{CAU}$-$\Psi_{27};f^5C_{34}$ for which higher fluctuations of 2.60 ± 0.60 were detected (Supplementary Data). The enhanced motional dynamics may be important for the decoding of AUA, as well as AUG.

The $tRNA^{Met}$ anticodon CAU is a cognate pair for the Met codon AUG. According to Crick's Wobble Hypothesis (36), the binding of anticodon **C**AU to codon AU**A** would be unlikely due to the C-A mismatch at the wobble position (wobble pair nucleosides in bold). However, the mitochondrial ribosome decodes both AUG and AUA using one tRNA with the anticodon CAU. This one tRNA consists of the modification f^5C_{34}. In contrast, two tRNAs decode the one Met codon AUG in the cytoplasm (37). One of the tRNAs is an initiator tRNA that decodes AUG in the ribosome's peptidyl- or P-site at the initiation of translation, where AUG is the first codon to be translated on the mRNA. This initiator $tRNA^{Met}_{CAU}$ consists of an unmodified CAU anticodon. The second cytoplasmic $tRNA^{Met}_{CAU}$ is responsible for elongation and recognizes AUG located within the mRNA, and thus responds only to the aminoacyl- or A-site codon. In *E. coli*, this elongator $tRNA^{Met}$ is modified with N4-acetylcytidine at the wobble position (ac^4C_{34}) (38). Thus, at the anticodon, one of the main distinguishing factors between the cytoplasmic initiator and elongator $tRNA^{Met}_{CAU}$ is the modification at the wobble position. We used a codon-binding assay to observe the affinity of the $hmASL^{Met}_{CAU}$-Ψ_{27}; f^5C_{34} and $hmASL^{Met}_{CAU}$-Ψ_{27} for the codons AUA and AUG at either A-site or P-site of *E. coli* 70S ribosomes. To ensure binding of the two ASL^{Met}s to the A- or the P-site, the ribosomal site not in observation (P- or A-site, respectively) was saturated with the unmodified *E. coli* ASL^{Val3}_{UAC} in response to its cognate codon GUA. The unmodified ASL^{Val3}_{UAC} binds its cognate codon with high affinity and specificity (39).

The $hmASL^{Met}_{CAU}$-Ψ_{27} bound AUG in the A-site and the P-site with an affinity comparable to what have observed previously for certain ASLs with unmodified wobble positions responding to cognate codons (Figure 6) (21,39). In contrast, the $hmASL^{Met}_{CAU}$-Ψ_{27} bound poorly to AUA in both the A- and P-sites. Surprisingly, introduction of f^5C_{34} enhanced binding to AUA by 2-fold (Figure 6). Our results indicated that of the two codons at either of the two ribosomal sites, the f^5C_{34} modification appears to be most important for reading AUA.

Both the $hmASL^{Met}_{CAU}$-Ψ_{27} and the fully modified $hmASL^{Met}_{CAU}$-$\Psi_{27};f^5C_{34}$ exhibited considerable affinity for AUG, and at both the A-site and the P-site. However, only the $hmASL^{Met}_{CAU}$-$\Psi_{27};f^5C_{34}$ exhibited significant affinity for AUA. There was a doubling in the affinity of ASL^{Met} for the AUA codon when f^5C_{34} was present. This increase in affinity of the f^5C_{34}-modified ASL in comparison to that of the $hmASL^{Met}_{CAU}$-Ψ_{27}, unmodified at the wobble position, was not observed on AUG and may therefore be the sole contributor to the efficient translation of AUA codons. A 2-fold increase in affinity of tRNA toward a codon has been shown to be significant in translation (40). Although some ASL modifications cause small increases in codon-binding affinity, others can dramatically increase affinity to codons (39).

Of particular interest is the chemical and conformational mechanisms by which a stable, but noncanonical base pair occurs between f^5C_{34} and the third base of the AUA codon, an adenosine, on the ribosome. C-A base pairs are extremely unusual. Although the C-A pairing has been found in the folded structure of some RNAs such as ribosomal RNAs (rRNAs), it is rarely found in anticodon:codon pairs. An anticodon:codon C-A mismatch has been detected when C_{34} of $tRNA^{Ile}_{CAU}$, modified with lysidine (k^2C_{34}) at the wobble position, is paired to the cytoplasmic isoleucine codon AUA. The lysine moiety of C_{34} on the anticodon provides an amino group which hydrogen bonds to A of the codon, thus allowing the wobble position C-A mismatch to occur. One could imagine that the 5-formyl modification raises the pK_a of cytidine's N3 to the physiological range where an additional hydrogen bond could be formed to AUA. However, the pK_a of f^5C determined by UV spectral analysis was lower than that of C (2.3 and 4.2, respectively; Figure 7), corresponding well with previous determinations (41) including those for df^5C (42) and for f^5U (43). Thus, f^5C must contribute to the decoding of the mitochondrial genome through a different mechanism. Another C-A anticodon:codon mismatch may occur at the wobble position when $tRNA^{Leu}_{f\,CmAA}$ pairs with the leucine codon UUA. Similar to $hmtRNA^{Met}$, this $tRNA^{Leu}$ isoacceptor has a 5-formylated, 2′-O-methylated C at the wobble position, f^5Cm_{34}. The wobble modifications are thought to be a general characteristic of mammalian cytoplasmic $tRNA^{Leu}$ that may aid in the decoding of leucine codons UUG and UUA and prevent the miscoding of the similar codons of phenylalanine, UUU and UUC. However, there is a lack of information on the decoding properties of $tRNA^{Leu}_{f^5CmAA}$ and therefore, there is the possibility that an isoacceptor other than $tRNA^{Leu}_{f^5CmAA}$ is responsible for specifically reading UUA (6,38).

Eighty percent of the methionine codons internal to mitochondrial mRNA are the AUA codon. Thus, the enhanced affinity of $hmASL^{Met}_{CAU}$-Ψ_{27};f^5C_{34} for AUA in the A-site of the *E. coli* ribosome has important implications for the affinity and kinetics of decoding AUA during elongation. The enhanced A-site binding of AUA by the f^5C-modified, $hmASL^{Met}_{CAU}$ may be even more evident on the mitochondrial ribosome, a concept not studied here. Also, the disease-related A37-G37 (A4435G) mutation, associated with an increased penetrance and expression of the primary Leber hereditary optic neuropathy mutation (G11778A), LHON (44), may critically alter the anticodon architecture such that either or both decoding events do not occur. This has yet to be examined. The synthesis of the wild-type modified and unmodified anticodon stem and loops of the $hmASL^{Met}_{CAU}$ and their physical, chemical characterizations will be important in understanding the contributions of the modification to biological function and in characterization of the human disease-relevant mutant tRNA.

SUPPLEMENTARY DATA

Supplementary Data are available at NAR Online.

ACKNOWLEDGEMENTS

We are very grateful to Dr. Glenn Björk (University of Umeå, Sweden) for the HPLC analysis of the synthesized RNA. AD is a Beckman Young Investigator and a Cottrell Scholar. We thank Mr. Antonio M. Munoz for his contribution to the molecular dynamics simulations.

FUNDING

The North Carolina State University RNA Biology Group (to A.D.); a grant from United Mitochondrial Disease Foundation, jointly with Dr. Linda Spremulli of the University of North Carolina–Chapel Hill (grant number 05-20 to P.F.A.); NSF (grant number MCB0548602 to P.F.A.); an NSF Graduate Fellowship (to E.M.G); and Dharmacon RNA Technologies, Inc. (ThermoFisher, Inc.). Funding for open access charge: National Science Foundation.

Conflict of interest statement. The perception of conflict may arise due to Drs. Michael O. Delaney and Rob Kaiser being employees of Dharmacon RNA Technologies (ThermoFisher). The company provided the polymer synthesis in which the f5C nucleotide was incorporated into RNA for the first time.

REFERENCES

1. Anderson,S., Bankier,A.T., Barrell,B.G., de Bruijn,M.H., Coulson,A.R., Drouin,J., Eperon,I.C., Nierlich,D.P., Roe,B.A., Sanger,F. *et al.* (1981) Sequence and organization of the human mitochondrial genome. *Nature*, **290**, 457–465.
2. Enns,G.M. (2003) The contribution of mitochondria to common disorders. *Mol. Genet. Metab*, **80**, 11–26.
3. Wittenhagen,L.M. and Kelley,S.O. (2003) Impact of disease-related mitochondrial mutations on tRNA structure and function. *Trends Biochem. Sci.*, **28**, 605–611.
4. King,M.P., Koga,Y., Davidson,M. and Schon,E.A. (1992) Defects in mitochondrial protein synthesis and respiratory chain activity segregate with the tRNA(Leu(UUR)) mutation associated with mitochondrial myopathy, encephalopathy, lactic acidosis, and strokelike episodes. *Mol. Cell Biol.*, **12**, 480–490.
5. Lombes,A., Bories,D., Girodon,E., Frachon,P., Ngo,M.M., Breton-Gorius,J., Tulliez,M. and Goossens,M. (1998) The first pathogenic mitochondrial methionine tRNA point mutation is discovered in splenic lymphoma. *Hum. Mutat.*, **(Suppl 1)**, S175–S183.
6. Pais de Barros,J.P., Keith,G., El Adlouni,C., Glasser,A.L., Mack,G., Dirheimer,G. and Desgres,J. (1996) 2′-O-methyl-5-formylcytidine (f5Cm), a new modified nucleotide at the 'wobble' of two cytoplasmic tRNAs Leu (NAA) from bovine liver. *Nucleic Acids Res.*, **24**, 1489–1496.
7. Moriya,J., Yokogawa,T., Wakita,K., Ueda,T., Nishikawa,K., Crain,P.F., Hashizume,T., Pomerantz,S.C., McCloskey,J.A., Kawai,G. *et al.* (1994) A novel modified nucleoside found at the first position of the anticodon of methionine tRNA from bovine liver mitochondria. *Biochemistry*, **33**, 2234–2239.
8. Watanabe,Y., Tsurui,H., Ueda,T., Furushima,R., Takamiya,S., Kita,K., Nishikawa,K. and Watanabe,K. (1994) Primary and higher order structures of nematode (Ascaris suum) mitochondrial tRNAs lacking either the T or D stem. *J. Biol. Chem.*, **269**, 22902–22906.
9. Tomita,K., Ueda,T. and Watanabe,K. (1997) 5-formylcytidine (f5C) found at the wobble position of the anticodon of squid mitochondrial tRNA(Met)CAU. *Nucleic Acids Symp. Ser.*, 197–198
10. Takemoto,C., Ueda,T., Miura,K. and Watanabe,K. (1999) Nucleotide sequences of animal mitochondrial tRNAs(Met)

possibly recognizing both AUG and AUA codons. *Nucleic Acids Symp. Ser.*, 77–78
11. Tomita,K., Ueda,T., Ishiwa,S., Crain,P.F., McCloskey,J.A. and Watanabe,K. (1999) Codon reading patterns in Drosophila melanogaster mitochondria based on their tRNA sequences: a unique wobble rule in animal mitochondria. *Nucleic Acids Res.*, **27**, 4291–4297.
12. Takemoto,C., Koike,T., Yokogawa,T., Benkowski,L., Spremulli,L.L., Ueda,T.A., Nishikawa,K. and Watanabe,K. (1995) The ability of bovine mitochondrial transfer RNAMet to decode AUG and AUA codons. *Biochimie*, **77**, 104–108.
13. Youssif,S., Mohamed,E.K., Ahmed,A.F.S. and Ghoneim,A.A. (2005) Synthesis of some new cytidine derivatives. *Afinidad*, **62**, 242–248.
14. Jurczyk,S.C., Kodra,J.T., Rozzell,J.D., Benner,S.A. and Battersby,T.R. (1998) Synthesis of oligonucleotides containing 2′-deoxyisoguanosine and 2′-deoxy-5-methylisocytidine using phosphoramidite chemistry. *Helv. Chim. Acta*, **81**, 793–811.
15. Scaringe,S.A., Kitchen,D., Kaiser,R.J. and Marshall,W.S. (2007) Preparation of 5′-silyl-2′-orthoester ribonucleosides for use in oligoribonucleotide synthesis. *Curr. Protoc. Nucleic Acid Chem.*, 2004 May; Chapter 2: Unit 2 10.
16. Hartsel,S.A., Kitchen,D.E., Scaringe,S.A. and Marshall,W.S. (2005) RNA oligonucleotide synthesis via 5′-silyl-2′-orthoester chemistry. *Methods Mol. Biol.*, **288**, 33–50.
17. Gehrke,C.W., Kuo,K.C., McCune,R.A., Gerhardt,K.O. and Agris,P.F. (1982) Quantitative enzymatic hydrolysis of tRNAs: reversed-phase high-performance liquid chromatography of tRNA nucleosides. *J. Chromatogr.*, **230**, 297–308.
18. Guenther,R.H., Gopal,D.H. and Agris,P.F. (1988) Purification of transfer RNA species by single-step ion-exchange high-performance liquid chromatography. *J. Chromatogr.*, **444**, 79–87.
19. Zumwalt,R.W., Kuo,K.C.T., Agris,P.F., Ehrlich,M. and Gehrke,C.W. (1982) High performance liquid chromatography of nucleosides in RNA and DNA. *J. Liquid Chromatogr.*, **5**, 2041–2060.
20. Ashraf,S.S., Guenther,R.H., Ansari,G., Malkiewicz,A., Sochacka,E. and Agris,P.F. (2000) Role of modified nucleosides of yeast tRNA(Phe) in ribosomal binding. *Cell Biochem. Biophys.*, **33**, 241–252.
21. Yarian,C.S., Basti,M.M., Cain,R.J., Ansari,G., Guenther,R.H., Sochacka,E., Czerwinska,G., Malkiewicz,A. and Agris,P.F. (1999) Structural and functional roles of the N1- and N3-protons of psi at tRNA's position 39. *Nucleic Acids Res.*, **27**, 3543–3549.
22. Serra,M.J. and Turner,D.H. (1995) Predicting thermodynamic properties of RNA. *Methods Enzymol.*, **259**, 242–261.
23. McCrate,N.E., Varner,M.E., Kim,K.I. and Nagan,M.C. (2006) Molecular dynamics simulations of human tRNA Lys,3 UUU: the role of modified bases in mRNA recognition. *Nucleic Acids Res.*, **34**, 5361–5368.
24. Jorgensen,W.L., Chandrasekhar,J., Madura,J. and Klein,M.L. (1983) Comparison of simple potential functions for simulating liquid water. *J. Chem. Phys.*, 926–935.
25. Fahlman,R.P., Dale,T. and Uhlenbeck,O.C. (2004) Uniform binding of aminoacylated transfer RNAs to the ribosomal A and P sites. *Mol. Cell*, **16**, 799–805.
26. Mathews,D.H., Turner,D.H. and Zuker,M. (2007) RNA secondary structure prediction. *Curr. Protoc. Nucleic Acid Chem.*, 2007 Mar; Chapter 11: Unit 11 2.
27. Phelps,S.S., Jerinic,O. and Joseph,S. (2002) Universally conserved interactions between the ribosome and the anticodon stem-loop of A site tRNA important for translocation. *Mol. Cell*, **10**, 799–807.
28. Wong,I. and Lohman,T.M. (1993) A double-filter method for nitrocellulose-filter binding: application to protein-nucleic acid interactions. *Proc. Natl Acad. Sci. USA*, **90**, 5428–5432.
29. Notari,R.E., Witiak,D.T., DeYoung,J.L. and Lin,A.J. (1972) Comparative kinetics of cytosine nucleosides. Influence of a 6-methyl substituent on degradation rates and pathways in aqueous buffers. *J. Med. Chem.*, **15**, 1207–1214.
30. Abdel Rahman,A.A.H., Wada,T. and Saigo,K. (2001) Facile methods for the synthesis of 5-formylcytidine. *Tetrahedron Lett.*, **42**, 1061–1063.
31. Bax,A., Griffey,R.H. and Hawkins,B.L. (1983) Correlation of proton and N-15 chemical shifts by multiple quantum NMR. *J. Magn. Reson.*, **55**, 301–315.
32. Bax,A. and Subramanian,S. (1986) Sensitivity-enhanced two-dimensional heteronuclear shift correlation NMR-spectroscopy. *J. Magn. Reson*, **67**, 565–569.
33. Wuthrich,K. (1986) *NMR of Proteins and Nucleic Acids*. Wiley-Interscience, New York, NY.
34. Jeener,J., Meier,B.H., Bachmann,P. and Ernst,R.R. (1979) Investigation of exchange processes by two-dimensional NMR spectroscopy. *J. Chem. Phys*, **69**, 4546–4553.
35. Case,D.A., Cheatham,, T.E. III. Darden,T., Gohlke,H., Luo,R., Merz,K.M. Jr, Onufriev,A., Simmerling,C., Wang,B. and Woods,R.J. (2005) The Amber biomolecular simulation programs. *J. Comput. Chem.*, **26**, 1668–1688.
36. Crick,F.H.C. (1966) Codon–anticodon pairing: the wobble hypothesis. *J. Mol. Biol.*, **19**, 548–555.
37. Mayer,C., Stortchevoi,A., Kohrer,C., Varshney,U. and RajBhandary,U.L. (2001) Initiator tRNA and its role in initiation of protein synthesis. *Cold Spring Harb. Symp. Quant. Biol.*, **66**, 195–206.
38. Sprinzl,M. and Vassilenko,K.S. (2005) Compilation of tRNA sequences and sequences of tRNA genes. *Nucleic Acids Res.*, **33**, D139–D140.
39. Vendeix,F.A., Dziergowska,A., Gustilo,E.M., Graham,W.D., Sproat,B., Malkiewicz,A. and Agris,P.F. (2008) Anticodon domain modifications contribute order to tRNA for ribosome-mediated codon binding. *Biochemistry*, **47**, 6117–6129.
40. Kurata,S., Weixlbaumer,A., Ohtsuki,T., Shimazaki,T., Wada,T., Kirino,Y., Takai,K., Watanabe,K., Ramakrishnan,V. and Suzuki,T. (2008) Modified uridines with C5-methylene substituents at the first position of the tRNA anticodon stabilize U.G wobble pairing during decoding. *J. Biol. Chem.*, **283**, 18801–18811.
41. Kawai,G., Yokogawa,T., Nishikawa,K., Hashizume,T., McCloskey,J.A., Yokoyama,S. and Watanabe,K. (1994) Conformatzonal properties of a novel modified nucleoside, 5-formylcytidine, found at the first position of the anticodon of bovine mitochondrial $tRNA^{Met}$. *Nucleosides Nucleotides*, **13**, 1189–1199.
42. Yoshida,M., Makino,K., Morita,H., Terato,H., Ohyama,Y. and Ide,H. (1997) Substrate and mispairing properties of 5-formyl-2′-deoxyuridine 5′-triphosphate assessed by in vitro DNA polymerase reactions. *Nucleic Acids Res.*, **25**, 1570–1577.
43. Karino,N., Ueno,Y. and Matsuda,A. (2001) Synthesis and properties of oligonucleotides containing 5-formyl-2′-deoxycytidine: in vitro DNA polymerase reactions on DNA templates containing 5-formyl-2′-deoxycytidine. *Nucleic Acids Res.*, **29**, 2456–2463.
44. Qu,J., Li,R., Zhou,X., Tong,Y., Lu,F., Qian,Y., Hu,Y., Mo,J.Q., West,C.E. and Guan,M.X. (2006) The novel A4435G mutation in the mitochondrial tRNAMet may modulate the phenotypic expression of the LHON-associated ND4 G11778A mutation. *Invest Ophthalmol. Vis. Sci.*, **47**, 475–483.